



ELSEVIER

Physica A 311 (2002) 97–110

PHYSICA A

www.elsevier.com/locate/physa

Observations of the effects of particle shape and particle size distribution on avalanching of granular media

D.A. Robinson*, S.P. Friedman

*The Institute of Soil, Water and Environmental Science, (ARO) The Volcani Center,
Bet Dagan, Israel*

Received 4 March 2002

Abstract

Measurements are presented for the angle of repose (α_r) and the maximum angle of stability (α_m) of a slope of poured granular material. Results using monosized grains with three materials of differing shape are presented. This is followed by results with binary mixtures. The results demonstrate a strong relationship between the slope angles and particle shape and that particle size distribution affects the slope angle and avalanching mode, especially as the grains become less spherical. © 2002 Elsevier Science B.V. All rights reserved.

PACS: 81.05.Rm

Keywords: Granular materials; Avalanching; Slope angle; Particle shape; Particle size distribution

1. Introduction

Granular materials pose interesting physical problems due to their behavior neither as a fluid nor a solid but as a somewhat intermediate phase. Recent theoretical [1–4] and experimental [5,6] studies have investigated some of the complex physics underlying these phenomena. During the pouring of a monosized granular material the heap formed is characterized by two angles, the angle of repose (α_r) and the maximum angle of stability (α_m) [7]. During the continuous pouring of a granular material the slope angle oscillates between the two values the former being the lower bound and the latter being the upper bound.

* Corresponding author. Present address: US Salinity Lab USDA-ARS, 450 W Big Springs Road, Riverside, CA, 92507, USA.

The importance of understanding slope dynamics is of crucial importance in both natural and industrial environments. Prediction of large-scale events such as rock falls and snow and ice avalanches is a prime concern in mountainous areas and requires an understanding of slope dynamics [8]. Marine avalanches can cut through underwater communication cables that are costly to repair. In storage silos the flow of granular materials has been known to cause stress failure in the silo structure [9]. The mixing and movement of all forms of industrial powders requires knowledge of granular flow [10]. Hence, a good physical understanding of slope stability and granular flow is important.

A fundamental challenge is to be able to predict the slope angles of a poured granular material. A variety of modeling methods have been used to investigate slope angles, all of which vary in their complexity. The simplest perhaps is a geometric model proposed by Barabasi et al. [11] based on a simple stability criterion, suggesting that the maximum angle of stability for spheres should be 23.4° . Other approaches are more complex and involve computer simulation such as the Monte Carlo (MC) method [12] or the distinct element method (DEM) [1,13]. In this paper we present a series of careful measurements of the angle of repose and maximum angle of stability of granular media. We investigate the role of particle shape using monosize materials and the effect of particle size distribution using binary mixtures of materials. Our hope is that the measurements will present challenges to theoreticians and can be used to test the predictive ability of different models.

2. Experimental design

2.1. Measurement cell

A range of methods are available for measuring the slope angle of materials [14]. A heap may be formed by pouring the material through a funnel, where as the crater method allows the material to drain from a beaker with a small drain hole in the center of the base, the disadvantage being that this only allows a measurement of the repose angle. Various revolving drum methods have been used [7] as well as confining the material between plates in a Hele–Shaw cell.

The Hele–Shaw cell was chosen as this allows observation of processes inside the slope structure. A diagram of the cell constructed from plexiglas is presented in Fig. 1. Improved delivery of the granular material ensuring an even slope in the cell was achieved with the use of a delivery slope placed at an angle of about 30° with a gate at the top. The height of the gate could be adjusted to alter the delivery rate.

The dimensions of the cell are important as the sidewalls can interact with the grains. Work presented [15] for binary mixtures of sugar and sand for example demonstrated that the mixing and segregation of material within a Hele–Shaw cell depended on both the separation of the sidewalls and the flow rate of the granular media into the cell. Koeppel et al. [15] found surprisingly that at certain flow rates and sidewall separations the media would segregate and form stratified layers within the slope. Based on

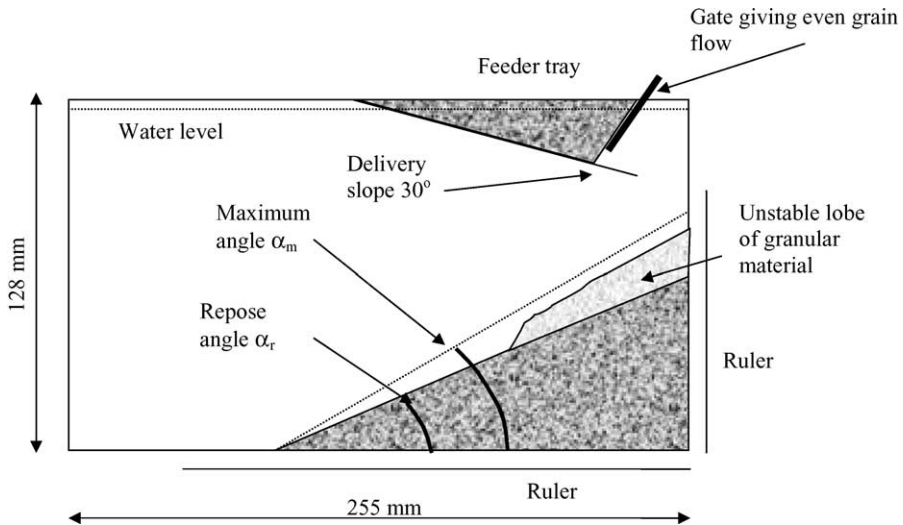


Fig. 1. Schematic diagram of the Hele–Shaw cell used to measure the slope angles showing the angle of repose (α_r) and the maximum angle of stability (α_m) which were measured.

these findings we chose a spacing of 30 mm, well outside the range where interaction with the sidewalls was observed to affect the measured slope angles.

2.2. Slope angle measurements

The construction of the Hele–Shaw cell in Plexiglas was straightforward, however, initial experimental results conducted with dry media, highlighted several problems. The Plexiglas created a static electric charge that affected the flow of the dry grains and even the use of an anti-static spray could not satisfactorily overcome this. More importantly, it was found that the momentum of the grains falling onto the pile obliterated the top of the slope making the slope angle difficult to measure accurately. Reducing the flow rate of the grains to reduce the momentum transfer by reducing the gate aperture caused clogging when using larger grains, which again created an uneven flow of grains. These problems were overcome by conducting the experiments under water as we considered that buoyancy would reduce the speed of the grains and their momentum transfer. This also removed the problem of electrostatic binding and reduced the friction between the grains and the gate aperture, hence giving an even flow. The use of water allowed for the creation of a well-defined slope and was found to work well in the particle size range from 100 and 500 μm . However, particles less than 100 μm were influenced by the currents that developed in the cell caused by the flow of the grains. This approach therefore, is not suitable for materials < 100 μm in diameter.

3. Experiments

3.1. Materials

Three granular materials were used in this study, glass beads (Mo-Sci Corp., Rolla, MO, USA), quartz grains (Yerucham Crater, Negev desert, Israel) and tuff grains (The Golan Heights, Israel). The particle size classes and some physical characteristics are presented in Table 1. All the materials were prepared in the laboratory by washing in de-ionized water, the quartz grains were also acid-washed to remove oxide coatings, they were all sieved to separate them into particle size classes. Pictures of the three materials are presented in Fig. 2. The shape factors for these materials were determined by digitally photographing (Aplitic Lis 700 camera) 30 particles under a microscope at $\times 40$ magnification. The digital images were analyzed to determine the circularity and sphericity using the Sigma Scan image analysis software, with each pixel representing $2.3 \mu\text{m}$.

Table 1
Physical characteristics of the materials used in the study

	Glass beads	Quartz grains	Tuff grains
Particle density (g cm^{-3})	2.48	2.65	2.88
Particle size classes (μm)			
Large ———	425–500	425–500	425–500
Medium ———	180–200		
Small ———	90–106	100–140	90–106
Very small ———	45–51		
Sphericity ^a (S)	1.00	0.73 (± 0.09)	0.59 (± 0.10)
Circularity ^b (C_i)	1.00	0.78 (± 0.04)	0.60 (± 0.08)

^aEq. (1).

^bEq. (2).

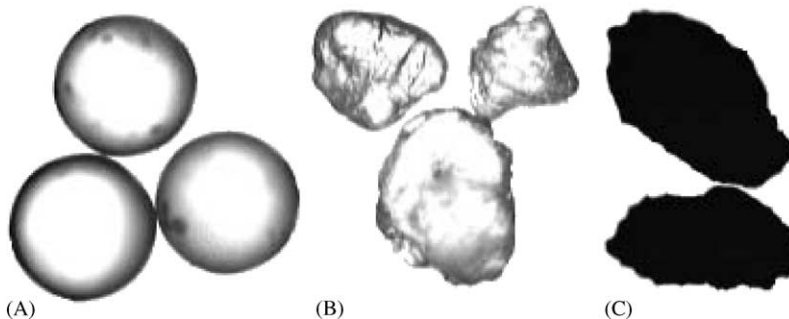


Fig. 2. Microscope photographs of A, glass beads, B, quartz sand grains and C, tuff grains. All grains approximately $500 \mu\text{m}$ in diameter.

3.2. Particle shape experiments

3.2.1. Slopes of particles with different shapes

The aperture size controlling the grain flow was adjusted to a suitable position so that flow-rates of about 0.4 gs^{-1} were achieved. Once a periodical steady state of accumulation and collapse was reached measurements of the maximum and repose angles were taken. In general, measurements were taken once a slope had reached at least 50 mm in length. The height and length could be measured to $\pm 0.5 \text{ mm}$ keeping the maximum error in the measurement of the slope angle to $\pm 0.5^\circ$, as the slope became longer this error reduced. Measurements of the angles formed by each mixture were the average of 10 or more sequential avalanches.

3.2.2. Mixtures of spheres with non-spherical particles

The slope angles of mixtures of particles of different shapes were obtained with glass spheres and quartz sand grains. Five mixtures were tested with volume fractions of sand of 0.09, 0.26, 0.33, 0.51 and 0.66; both the maximum and repose angles were measured.

3.3. Particle size distribution experiments

3.3.1. Monosize spheres

The initial step was to experimentally determine the influence of the size of the particles on the slope angles within the size range between 50 and 500 μm . Contradictory findings can be found in the literature for particles of $< 1 \text{ mm}$ in diameter, some suggesting there is an effect [16,17] and some having observed no effect [7]. Certainly as particles become smaller the charge/mass ratio increases. This means that at some particle size the electrostatic interaction will begin to contribute to the flowability of particles. Wong [18] observed a decrease in the aerated bulk density of glass spheres beginning at about 60–70 μm . Glass beads with diameters of 50, 100, 200 and 500 were used to determine slope angles for monosize spheres. The 50 μm measurements were carried out in dry air (relative humidity of about 40%) as circulation currents prevented the formation of a measurable slope under water.

3.3.2. Binary mixtures

Binary mixtures of large (450–500 μm) and small (90–106 μm) grains were used to determine any effect of particle size distribution on the slope measurements. At least four different volume fraction ratios were used to augment the measurements conducted with monosized materials. A clear advantage of making the measurements in water now became apparent. The use of water allowed for thorough and homogeneous mixing of the two particle sizes by carefully controlling the water solid ratio above the gate in the measuring cell. Performing these measurements in air proved almost impossible, as the two particle sizes did not mix homogeneously.

4. Results and discussion

4.1. Particle shape

The quantification of the shape of grains is itself a challenging physical problem. Most methods rely on using a two-dimensional image of the particle. Wardell [19] proposed placing particles under a microscope and using the plan image to evaluate the particles maximum cross-sectional area. The contribution of gravity will generally ensure that the view is the maximal area. The area of this image of the grain (A_p) is then compared with the area of the smallest inscribed circle into which the grain fits in its entirety (A_c). In Wardell's [19] discussion of shape the ratio of the areas is defined as the sphericity (S):

$$S = \frac{A_p}{A_c}. \quad (1)$$

An alternative shape factor, the circularity (Ci) used in many image analysis programs [e.g. Sigma Scan Pro5] is defined as

$$Ci = \frac{4\pi A_p}{P^2}, \quad (2)$$

where, P is the length of the perimeter of the particle. Circularity has the advantage of incorporating a measure of the roughness or surface undulations of the particle, which the sphericity does not. However, the quality of the area determination will depend on the photograph quality and the fractal dimension of the grains surface. Both ratios are 1 for spheres and decline as the grains become less spherical.

Data for both experiments, Sections 3.2.1 and 3.2.2, are presented in Fig. 3 versus the circularity; the experiments presented used the 500 μm grains. Two curves are fitted to show the general trend in the data. One can clearly see a divergence between the maximum and repose angles as the particle shape becomes less spherical. The result for the maximum angle for the spheres $\alpha_m = 23.1$ fits well with the predicted value of 23.4 using a simple geometric model [11]. As one would intuitively expect the relationship should be non-linear, flattening out as the maximum slope values are obtained. There must be a finite value smaller than 90° above which, a stable slope of cohesionless particles cannot exist. The mixtures of spheres with sand grains appear to follow a small curvature very much in the general trend of the overall curvature with shape. Friedman and Robinson [20] have suggested that use could be made of this relationship between slope angle and grain shape such that the slope angle could be used as an estimate of the three-dimensional nature of the granular material. In that work slope angle was linked to ellipsoid depolarization factors, so that permittivity and electrical conductivity of saturated granular media could be predicted.

Although there appears to be a firm relationship between grain shape and the slope angle of the pile it is worth considering a note of caution. The use of a two-dimensional image to characterize the shape of three-dimensional particles presents its difficulties. The third dimension of the particle essentially remains an unknown. The particles could tend to be oblate if the unknown dimension is small, or prolate if the unknown dimension is similar to the width of the particle. In the case of the tuff grains used

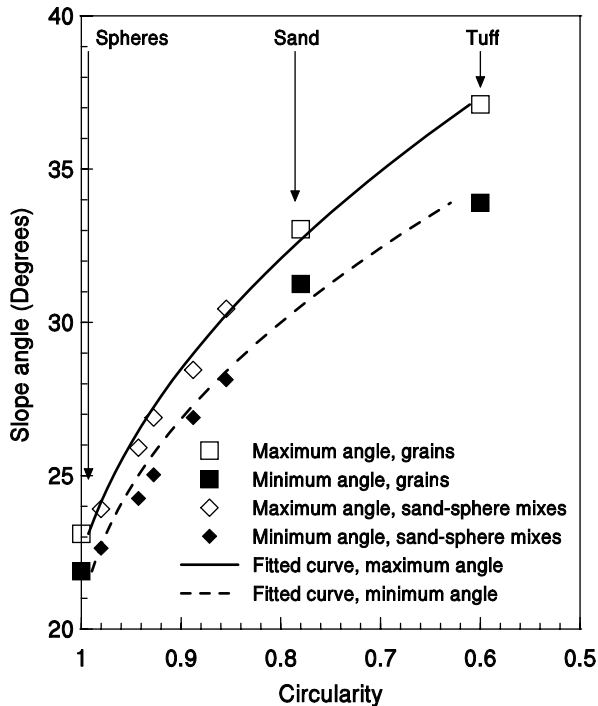


Fig. 3. Slope angles as a function of two-dimensional circularity. The data for mixtures represent sand of volume fraction 0.09, 0.26, 0.33, 0.51, 0.67 mixed in glass spheres.

in our experiment we attempted to measure this directly using a micrometer, the results showing the particles tend to oblate in shape. The curvature observed in Fig. 3 may be a function of the oblate/prolate nature of the particles and is worth further investigation.

4.2. Particle size

The results for the slopes of spheres of differing sizes are presented in Fig. 4. These results demonstrate no apparent influence of the size of the particles on the slope angles. This is in agreement with the findings of Jaeger et al. [7], who also found no apparent effect of the size of monosize glass spheres of 500 and 70 μm . It is likely that due to the increased electrostatic effect with decreasing particle size that there will come a point at which the slope angles may change as the gravitational and electrostatic forces interact. A study of this possible effect would be an interesting contribution to our understanding and the literature. High momentum transfer can have a considerable effect on the slope angle so that measurements that have decreasing slope angles as the particle size increases may be incorporating the effects of increased momentum

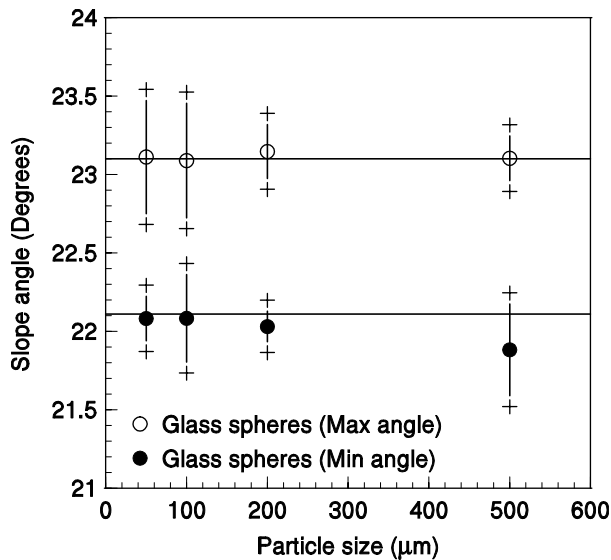


Fig. 4. Slope angle as a function of particle size for glass spheres, the crosses give 1 standard deviation. Particle sizes 100, 200 and 500 μm were conducted under water where as 50 μm was conducted in dry air.

transfer. The destructive impact of the larger particles tends to reduce the overall angle of the slope if only measured at the top and base of the slope.

The results of experiment, Section 3.3.2, are presented in Fig. 5. These measurements presented considerable experimental difficulty, especially with maintaining the uniform binary mixture. The results are subtle but we believe indicate a trend that is well worth further investigation. The data for binary mixtures (450–500 μm , large and 90–106 μm , small), compared with monosize (450–500 μm), show a subtle increase of the maximum angle of stability prior to slope collapse, as the volume of small grains was increased to approximately one-third. This was mirrored by a more significant effect on the corresponding angle of repose, most noticeably for a mixture with 0.2 small, as the shape became less spherical (Fig. 5c). The standard deviation reflects more than simply the repeatability of the measurements. For the 0.2 and 0.33 small in large it reflects different avalanche magnitudes, believed to be a function of the amount of percolation of the small particles. This suggests that the predictability of such events will become more difficult, the less uniform the system becomes. The value of approximately one-third small mixed in large is significant as this is the porosity minimum achieved within a binary packing where the void space between the large is efficiently filled by small. At this volumetric fraction of small particles the density of the slope increases as do the number of contact points between particles [21]. Fig. 5d shows the corresponding measured porosity change for a binary mixture of spheres, modeled using a fractional packing model [22] for the size ratio of 5. Above the porosity minimum the angles for all the materials converge to their values for monosize grains. It is clear from Figs. 5a–c that surface roughness properties and

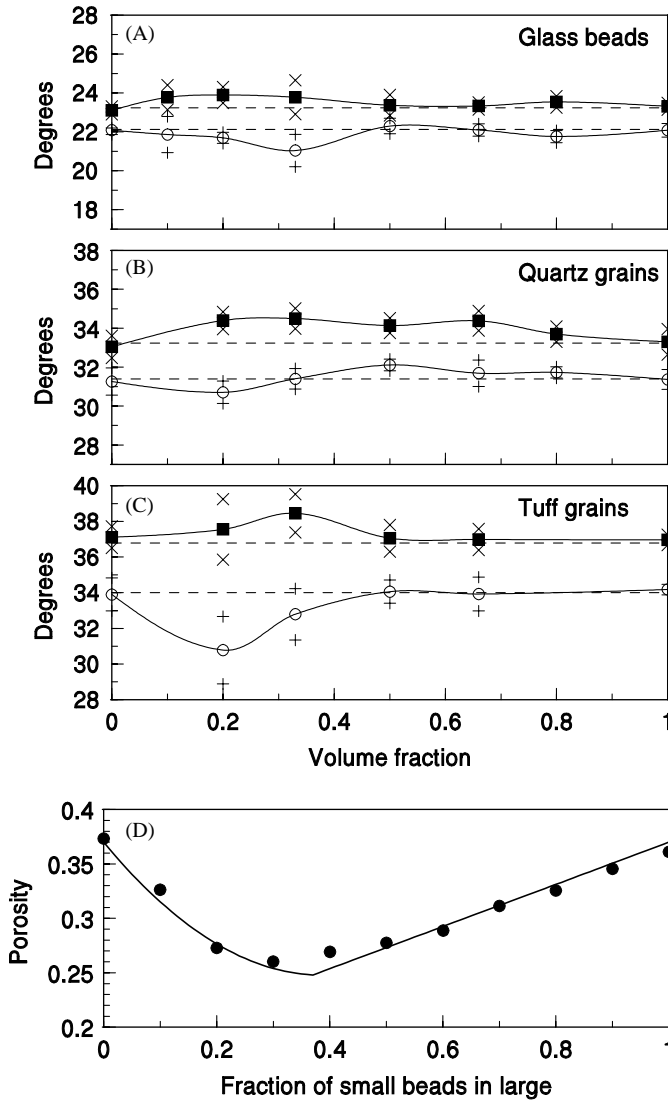


Fig. 5. (a–c). The maximum angle of stability and angle of repose for three binary mixtures of differing grain shapes, with the volume fraction of small grains mixed into large along the base. The crosses and plus signs mark one standard deviation and the dashed lines indicate the maximum and repose angles for comparison. (d). The porosity as modelled according to [22] for a size ratio of 5 with data presented for measurements with glass beads.

the deviation of the particles from the shape of a sphere has the greatest effect on the slope angles. However, the shape effect also strongly influences the binary mixtures so that an increase in the maximum and decrease in the minimum angles becomes greater as the shape becomes less spherical. In practical terms, the avalanches become

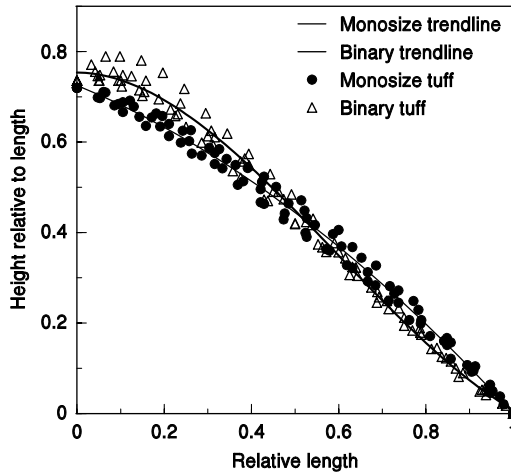


Fig. 6. The shape of material lobes formed on the slope prior to avalanching of the tuff. Note the difference in shape between the monosize material and a binary mixture containing $\frac{1}{3}$ small. The data is of lobes of varying length collected from sequential avalanches so that the length scale for the base is relative.

larger (maximal value of $\alpha_m - \alpha_r$) when the particles are rougher and more angular and composed of one-third small grains mixed in large.

We propose that a possible reason for the observed ‘mirroring’ of the maximum and minimum angles for binary mixtures is due in part to the increased amount of contact between grains in the slope for a given particle shape leading to arching [23,24]. Increased arching would allow an increased value of the maximum angle. The decreased angles of repose would then reflect the collapse of arches providing more energy for the avalanche, greater perturbation in turn generating thicker surface avalanches.

Morphological changes in the appearance of the slope were observed with the binary mixtures. These observations show subtle differences in the shape of the slope prior to reaching the maximum angle of stability. As the particles become less spherical we believe there are more contact points and increased wedging of the small angular grains between the large. This may help to strengthen and stabilize the slope and spread the stress loading. The observable results were a change in the morphology of the lobe of material (described in Fig. 1) causing the avalanche. After an avalanche had reduced the slope to its repose angle, a lobe of material would form at the top of the slope as fresh material was deposited (Fig. 1). At a critical point this lobe would collapse resulting in a thin, surface flow avalanche. The length of the lobe compared to the base of the slope generally lay between one-quarter and one-half its length. The shape of the lobes causing the avalanche for monosize and binary packing of tuff are presented in Fig. 6. The monosize lobe was distinctly convex (negative curvature) and at a critical point would burst from near the base as the mass increased above. The lobe formed by the binary mixture differed distinctly being convex towards the top and concave towards the base. This change of morphology as a result of the binary mixing

appeared to make a stronger and more stable lobe that contained more material than its monosize counterpart. Upon failure, the collapse of this lobe resulted in a larger surface avalanche.

The sequence of events building up to an avalanche starting from the point where the slope has just collapsed forming the angle of repose follow a distinctive pattern. A periodic build up and collapse of progressively larger lobes of material on the repose slope occurs. When these events have filled the area between the maximum angle and repose angle on Fig. 1 the whole slope collapses back to the repose angle. It is important to point out that the maximum angle and repose angle are measured at the point before collapse (α_m) and the point immediately after (α_r). These are the measurements referred to in this work and not the intermediate cases. The discussion of lobes refers to the intermediate case.

Segregation of binary mixtures forming banding within the slopes formed by avalanching has been observed with attempts being made to model it [15,25–27]. The fine grains tend to be trapped higher up the slope, more easily caught in crevices and with less energy to overcome them. The larger grains tend to roll over these and because they have greater size are less likely to be trapped in crevices. It was evident that during an avalanche the layer of small grains formed a bed, acting like small ball bearings, over which the large grains rolled. This mechanism accounts for the size segregation leading to banding during periodic accumulation and collapse. When grains of mixed size are sheared together the larger grains migrate to the zone of least shear strain, i.e., the surface, the smaller grains migrate towards the zone of greatest shear strain, the base of the flow [28].

We noticed however, that the segregation became less distinct as the quantity of small grains was reduced below one third and the small grains percolated through the large. Below 0.33 small beads, voids appear within the matrix as the quantity of small is insufficient to fill all the space between the large. This results in a pile with greater potential energy, as the small grains, which can form essentially the ‘keystone’ in a bridging structure, can, upon a small perturbation collapse into the voids.

To investigate the increased potential energy of a slope a qualitative experiment was conducted comparing slope dynamics of spherical particles with two different bases. A rough base is normally used in the experiments and the base of our Hele–Shaw cell had been scoured with coarse glass paper making it rough. This was then compared with an unaltered smooth plexiglas base, thereby reducing the friction between the surface of the cell and the particles supported by it. The results (Fig. 7) clearly demonstrate a much more unstable structure resulting from binary mixtures below the porosity minimum. Rather than a surface avalanche occurring as previously observed, the whole slope became unstable and slumped due to internal redistribution of the matrix. The internal point of failure of the slope appeared to occur about one third out from beneath the pile apex along the base. According to theoretical analysis [23] this is where the center of pressure is likely to be located for a pile of spherical grains. This qualitative experiment indicates the importance of the particle size composition of a slope in terms of its stability. The results contain implications for the engineering stability of slopes and we would suggest that further work might investigate this more thoroughly.

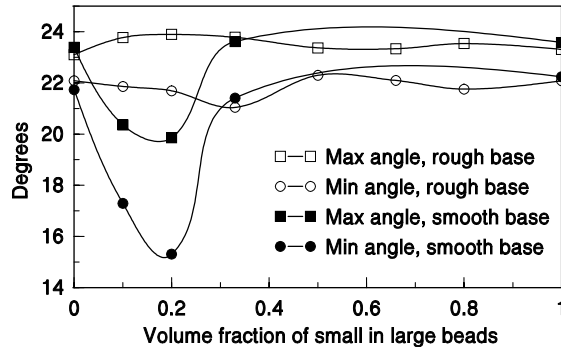


Fig. 7. The maximum angle of stability and angle of repose with the slope formed in the Hele–Shaw cell with a rough Plexiglas base and a smooth Plexiglas base which had less friction. The slope is far less stable below the porosity minimum when the structure contains voids.

The avalanche behavior of this type of slope differs markedly from that observed for surface avalanches. The diagram in Fig. 8 helps to visualize the differing processes between a pile with a stable base and one with an unstable base. Fig. 8a shows segregation formed by surface avalanching described earlier as the small spheres form the base of each sequential avalanche. Fig. 8b shows the differing internal structure of a slope on a smooth base. Fig. 8c is a photograph of this slope structure. The dark areas are the large grains and the light areas are the small ones. Small beads arriving at the top of the slope percolate through the large grains making their way quickly to the base of the pile. Others wedge between large grains forming bridges. When the bridges collapse the small beads fall into voids and again percolate to the base of the pile. A bed of small beads forms at the base of the pile, these act like ball bearings carrying the large beads. The structural collapse tends to be more catastrophic so that smaller values of repose angle result (Fig. 7) due to the rotational slip. With sequential slumping the small beads percolate and are pushed along the base of the pile. This results in a distinct ‘toe’ at the base of the slope made almost entirely of small beads. It is important to remember that these beads have percolated through the pile and not flowed down the slope. The resulting internal structure is very different to the banding formed by a stable or non-percolating pile with surface avalanches.

5. Conclusions

A careful set of measurements is presented that demonstrate the effect of particle shape and particle size distribution on both the angle of repose and the maximum angle of stability. Increased angularity of the grains increases the slope angle. The angle of repose and the maximum angle appear to mirror each other in magnitude as the volume fraction of small grains mixed in large increases. The maximum angle increases and the repose angle reduces, the greatest effect being observed at volume fractions between 0.2 and 0.3. Total slope failure and slumping was observed to occur for binary mixtures

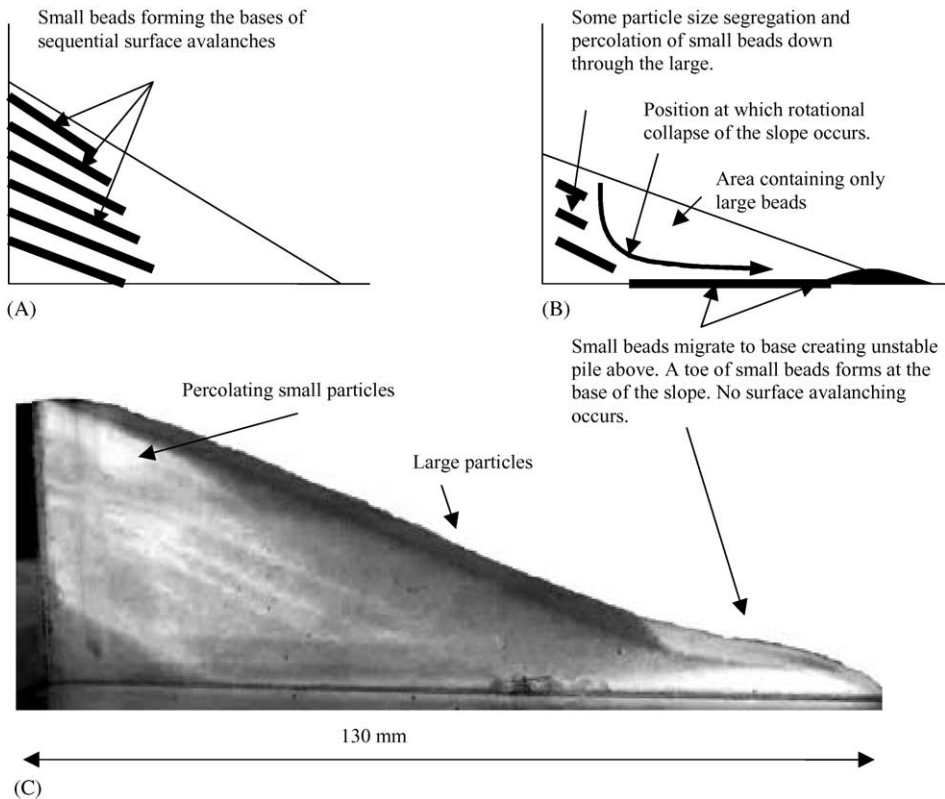


Fig. 8. Conceptual diagram of the internal structure of piles formed with binary mixtures containing 0.2 small grains. (A) The cell has a rough base and the pile is stable with oscillating surface avalanches, the differing particle sizes form segregation banding. (B) Small grains percolate down through the pile and collect along the base. The small beads form a ball bearing like surface over which the slope forms, as the overburden pressure increases to criticality the slope slumps and collapses. Very little surface avalanching occurs. (C) Photograph of slope corresponding to (B).

of spheres forming a slope on a smooth surface with volume fractions of small grains mixed in large lower than 0.3.

Acknowledgements

This research was supported in part by research Grant No. IS-2839-97, from BARD. The United States–Israel Binational Agricultural Research and Development Fund.

References

- [1] Y.C. Zhou, B.D. Wright, R.Y. Yang, B.H. Xu, A.B. Yu, *Physica A* 269 (1999) 536–553.
- [2] H.J. Herrmann, *Physica A* 263 (1999) 51–62.

- [3] J.P. Wittmer, M.E. Cates, P. Claudin, *J. Phys. 1 France* 7 (1997) 39–80.
- [4] P. Claudin, J.P. Bouchaud, M.E. Cates, J.P. Wittmer, *Phys. Rev. E* 57 (4) (1998) 4441–4457.
- [5] A. Daerr, S. Douady, *Nature* 399 (1999) 241–243.
- [6] Y. Grasselli, H.J. Herrmann, *Physica A* 246 (1997) 301–312.
- [7] H.M. Jaeger, C.-H. Liu, S.R. Nagel, *Phys. Rev. Lett.* 62 (1) (1989) 40–43.
- [8] I. Statham, *Sedimentology* 21 (1974) 149–162.
- [9] L. Vanel, Ph. Claudin, J.-Ph. Bouchaud, M.E. Cates, E. Clement, J.P. Wittmer, *Phys. Rev. Lett.* 84 (7) (2000) 1439–1442.
- [10] P.G. de Gennes, *Physica A* 261 (1998) 267–293.
- [11] A.-L. Barabasi, R. Albert, P. Schiffer, *Physica A* 266 (1999) 366–371.
- [12] R. Jullien, P. Meakin, *Nature* 344 (1990) 425.
- [13] Y.C. Zhou, B.H. Xu, A.B. Yu, P. Zulli, *Phys. Rev. E* 64 (1–8) (2001).
- [14] M.A. Carrigy, *Sedimentology* 14 (1970) 147–158.
- [15] J.P. Koeppe, M. Enz, J. Kakalios, *Phys. Rev. E* 58 (4) (1998) 4104–4107.
- [16] M.A. Qazi, *The Arabian J. Sci. Eng.* 1 (2) (1975) 69–78.
- [17] J.M. Sperry, J.J. Peirce, *Ground Water* 33 (1995) 892–898.
- [18] A. Wong Chi-Ying, *Chem. Eng. Sci.* 55 (2000) 3855–3859.
- [19] H. Wardell, *J. Geol.* 43 (1935) 250–280.
- [20] S.P. Friedman, D.A. Robinson. *Water Resources Res.*, 2002, submitted for publication.
- [21] R.P. Pinson D Zou, A.B. Yu, P. Zulli, M.J. McCarthy, *J. Phys. D* 31 (4) (1998) 457–462.
- [22] C.E. Koltermann, S.M. Gorelick, *Water Resources Res.* 31 (12) (1995) 3283–3297.
- [23] J.P. Wittmer, M.E. Cates, P. Claudin, *J. Phys. 1 France* 7 (1997) 39–80.
- [24] C.-H. Liu, S.R. Nagel, D.A. Schecter, S.N. Coppersmith, S. Majumdar, O. Narayan, T.A. Witten, *Science* 269 (1995) 513–515.
- [25] H.A. Makse, S. Havlin, P.R. King, H.E. Stanley, *Nature* 386 (1997) 379–382.
- [26] J. Baxter, U. Tuzun, D. Heyes, I. Hayati, P. Fredlund, *Nature* 391 (1998) 136.
- [27] H.J. Herrmann, *Physica A* 270 (1999) 82–88.
- [28] R.A. Bagnold, *Proc. Roy. Soc. London A* 225 (1954) 49–63.